Journal of the Korean Physical Society, Vol. 55, No. 5, November 2009, pp. 1887∼1891

MgO-Core/ZnO-shell Nanocables Sheathed by Using the Sputtering Technique

Hyoun Woo Kim, Hyo Sung Kim,* Chongmu Lee and Mesfin Abayneh Kebede
Division of Materials Science and Engineering, Inha University, Incheon 402-751

Keon-Ho Yoo
Department of Physics and Research Institute for Basic Science, Kyung Hee University, Seoul 130-701

Doo Young Kim
Department of Chemistry, Michigan State University, East Lansing, Michigan 48824, U.S.A.

(Received 2 September 2008)

We demonstrated the successful fabrication of MgO-core/ZnO-shell nanowires, in which the shell layers were deposited by using the sputtering technique. Transmission electron microscopy investigations revealed that core nanowires were surrounded by a ZnO shell layer. At 298 K, the photoluminescence (PL) peak intensity ratio (green/UV) decreased with increasing ZnO shell thickness. In regard to the effect of temperature, the intensity of the green emission band was progressively decreased with increasing measurement temperature. We discuss the possible associated PL emission mechanisms.

PACS numbers: 61.46.-w, 61.82.Fk, 68.37.Lp, 68.37.Hk, 78.55.-m
Keywords: MgO, ZnO, Plasma sputtering, Photoluminescence
DOI: 10.3938/jkps.55.1887

I. INTRODUCTION

One-dimensional (1D) nanostructures (such as wires, rods, and tubes) have been the focus of extensive research in recent years due to their potential applications in fabricating nanoscale electronic, optoelectronic, and sensing devices [1–8]. In order to realize various tailor-made functions, coaxial 1D structures with a core/sheath geometry have been created.

Magnesium oxide (MgO) has been an exceptionally important material for use in catalysis and toxic waste remediation and as an additive in refractory, paint and superconductor products [9–11]. Furthermore, MgO is a typical wide-bandgap insulator; thus, the electronic and the optical properties of bulk MgO have been investigated [12–14]. Accordingly, several researchers have reported on the synthesis of 1D MgO nanostructures [15, 16] however, they generally conducted their studies from the viewpoint of the preparation method and characterization. Zinc oxide (ZnO) is not only a promising material for ultraviolet (UV)/blue devices but also for spintronics if it is doped with magnetic impurities [17]. Furthermore, since ZnO is bio-safe and biocompatible, it can be used for biomedical applications [18,19].

In our attempt to fabricate MgO/ZnO core-shell nanowires in this study, we have used a sputtering technique with a ZnO target. A significant improvement of PL emission has been demonstrated in the ZnO/MgO core-shell quantum dots [20]. Furthermore, ZnO-MgO heterostructures have been useful in the study of chemical sensors, optical devices, scanning probes, and heterojunction materials with quantum confinement effects [21]. Up to the present, a variety of techniques including chemical vapor deposition (CVD) and the sol-gel process, have been employed. Compared to the CVD method, sputtering is more efficient, resulting in a high productivity. Compared to the sol-gel process, sputtering is more well-controllable and precise, which is suitable for future ULSI systems. To the best of the authors' knowledge, this is first report on the fabrication of ZnO sheaths by using a sputtering technique.

II. EXPERIMENTS

As a core material, MgO nanowires were synthesized by thermal heating of MgB_2 powders in a quartz tube. The pure MgB_2 powders were heated, and the associated vapors were deposited on Au-coated (3-nm-thick) Si substrates. The substrate temperature was set to 900 °C in

*E-mail: hwkim@inha.ac.kr; Fax: +82-32-862-5546

a flow of an O_2 /Ar gas mixture. The shell coating on the as-prepared MgO nanowires was performed using an RF sputter system, where schematic diagram was previously described [22]. A 70W RF power at a frequency of 13.56 MHz was supplied in an Ar (99.99 % purity) gas atmosphere The flow rates of the Ar and the O_2 gases were set to 30 and 10 sccm, respectively, at room temperature at a pressure of 5.0×10^{-2} Torr A 99.99 %-pure ZnO target was used and deposition was carried out for 2, 4, or 8 min.

The structural properties of the samples were analyzed by using glancing angle (0.5°) X-ray diffraction (XRD, Philips X'pert MRD diffractometer with CuKα_1 radiation), field emission scanning electron microscopy (FE-SEM Hitachi, S-4200), and transmission electron microscopy (TEM Philips, CM-200) with an energy dispersive X-ray spectroscopy (EDX) installed. The PL was measured with the 325nm line from a He-Cd laser. In additional experiments for investigating the temperature-dependence of the PL, the sample temperature was controlled from 18.8 K to 300 K by using a closed-cycle refrigeration system (Janis CCS-100) and a temperature controller (Lakeshore 330). The luminescent light was dispersed by using a 50-cm monochromator (Spex 500M) and was detected by using a cooled photomultiplier tube (ISA Jobin-Yvon R955). A lock-in amplifier (EG&G 5210) was used to increase the signal-to-noise ratio.

1. III. RESULTS AND DISCUSSION

Figures 1(a) and 1(b) show typical SEM images of MgO-core/ZnO-shell nanowires sputtered for 2 min and 8 min, respectively. The images clearly reveal that products consist of 1D structures, regardless of sputter time. Figure 1(c) shows an XRD pattern of MgO-core/ZnO-shell nanowires sputtered for 4 min. Some diffraction peaks can be indexed to the tetragonal rutile structure of MgO with lattice constants of $a = 4.738$ Å and $c = 3.187$ Å (JCPDS File No. 040829) from the core nanowires whereas other weak reflection peaks can be indexed as the hexagonal lattice of ZnO, which are in agreement with JCPDS file No. 05-0664. Accordingly, the XRD analysis reveals not only the inner core of cubic MgO but also the outer shell of hexagonal ZnO.

Figure 2(a) shows a TEM image of a MgO-core/ZnO-shell nanowire, consisting of a rod-like core and thin coating layers on both sides. The outer shell layers are continuous along the nanowire. The diameter of the core is approximately 75 nm whereas the thickness of the shell layer ranges from 25 to 35 nm. Figure 2(b) shows the selected area electron diffraction (SAED) pattern taken from the shell region of the coated nanowire, which appears to be a superposition of single crystal spot patterns arising from the polycrystalline nature of the ZnO shell. In addition, the pattern shows a halo in the center,

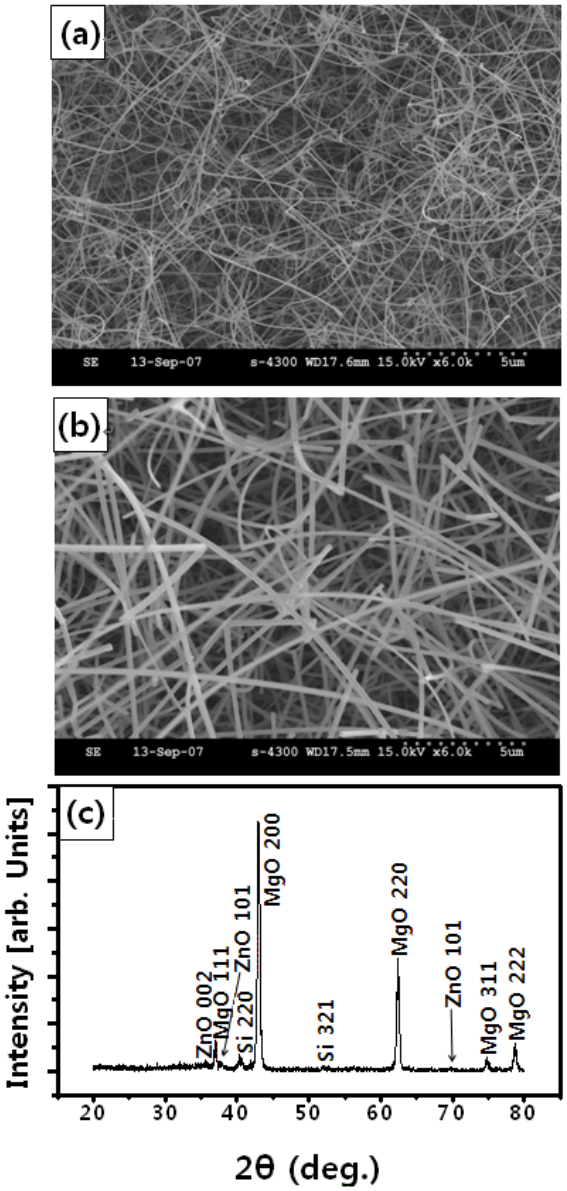

Fig. 1. SEM images of the MgO/ZnO core-shell nanowires sputtered for (a) 2 min and (b) 8 min. (c) XRD pattern of MgO/ZnO core-shell nanowires sputtered for 4 min.

suggesting the existence of an amorphous phase. An enlarged TEM image from the area enclosed by the dotted square in Figure 2(a) is shown in Figure 2(c). Visible lattice fringes are evidence that the shell layer is polycrystalline. The spacing between two adjacent lattice planes is about 0.25 nm, corresponding to the spacing of (101) planes in a hexagonal ZnO crystal. No dislocation line can be seen in this image. The EDX spectrum shown in Figure 2(d) indicates that the synthesized nanowires consist of Mg, Zn, and O elements. Since the core nanowires correspond to pure MgO, the existence of a Zn peak indicates that the shell layer is comprised of Zn elements.

Figures 3(a) and 3(b) show normalized PL spectra of

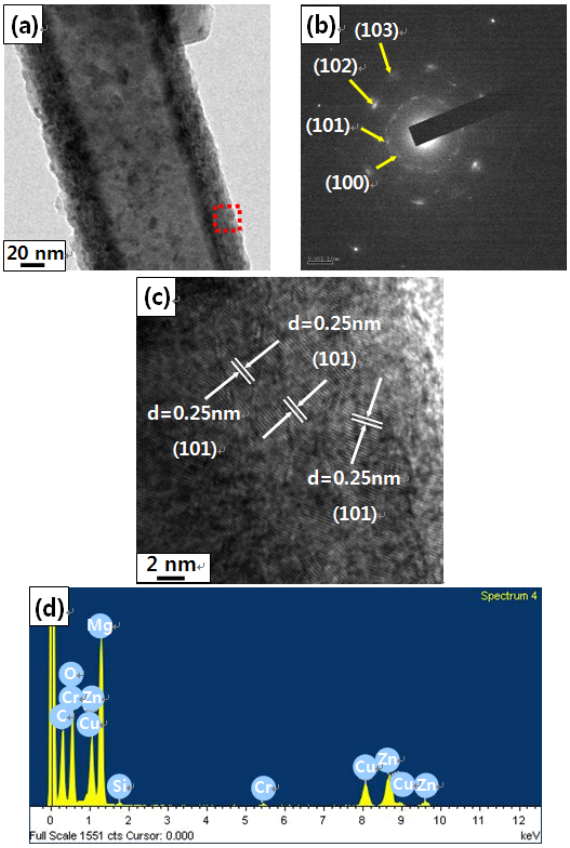

Fig. 2. (a) Representative TEM image of a MgO/ZnO core-shell nanowire sputtered for 4 min. (b) Corresponding SAED pattern. (c) Lattice-resolved TEM image enlarging the area enclosed by the dotted square in (a). (d) Corresponding TEM-EDX spectrum.

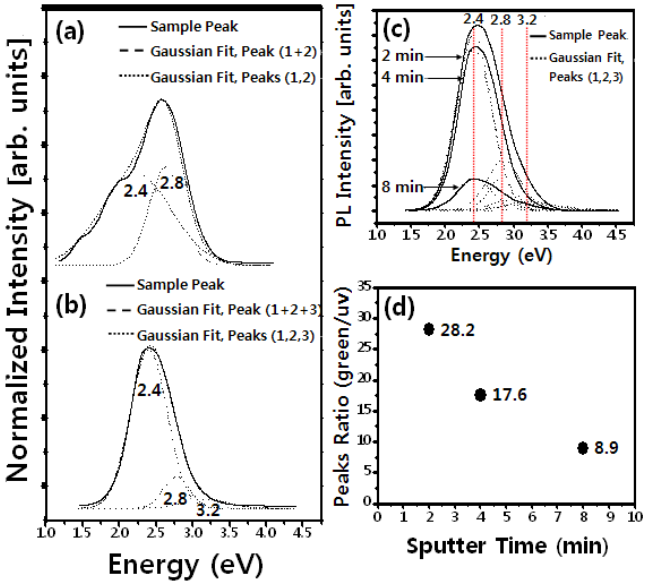

Fig. 3. Normalized PL spectra of (a) MgO core nanowires and (b) MgO/ZnO core-shell nanowires sputtered for 4 min. (c) Comparison of PL intensities of MgO/ZnO core-shell nanowires sputtered for 2, 4, and 8 min. (d) Variation of the green-to-UV peak intensity ratio for samples sputtered for 2, 4, and 8 min.

core and ZnO-coated MgO nanowires, respectively. A multi-peak Gaussian fitting analysis indicates that the spectrum in Figure 3(a) consists of two bands, peaking at approximately 2.4 eV in the green region and 2.8 eV in the blue region, respectively. The blue and the green emissions originate from defects in MgO [13,23], which could be generated during the hightemperature fabrication of MgO core nanowires. Figure 3(b) reveals three bands, peaking at 2.4 eV, 2.8 eV, and 3.2 eV, respectively. Besides the 2.8eV peak from MgO core, it is noteworthy that a 2.4 eV peak has been significantly intensified after the ZnO coating. We surmise that the green emission peak, which originates from the ZnO core and is known to be related to defects such as oxygen vacancies [24–27], has overlapped the existing green peak from the MgO core nanowires. In addition, the ultraviolet (UV) band (3.2 eV) is associated with the excitons in ZnO [24,25].

In order to compare the intensities, we have shown the PL spectra of MgO-core/ZnO-shell nanowires with sputter times of 2, 4, and 8 min, in Figure 3(c). While the Gaussian deconvolution analysis confirmed the existence of three bands (2.4 eV, 2.8 eV, and 3.2 eV) regardless of the sputter time, the overall PL intensity decreased with increasing thickness of the ZnO shell layer. For revealing the origin of this phenomenon, we present the luminescence peak intensity ratio (green (2.4 eV)/ UV (3.2 eV)) in Figure 3(d). The peak intensity ratio decreased with increasing ZnO shell thickness. This phenomenon is similar to that in the previous work, in which the green-to-UV peak ratio increased with increasing ZnO nanowire diameter [28] or increasing ZnO film thickness [29]. The progressive decrease on the peak ratio (green/UV) as the shell thickness increases suggests that there is a smaller fraction of oxygen vacancies in thicker shell layers [28]. We believe that the higher surface-area-to-volume ratio for thinner shell layers should favor a higher level of surface and sub-surface oxygen vacancies [28].

The temperature-dependent PL excited at 325 nm was investigated at temperatures ranging from 18.8 to 300 K (300, 200, 100, and 18.8 K) for the 8-min-sputtered sample and is shown in Figure 4(a). It is noteworthy that the overall PL intensity progressively increased with decreasing measurement temperature. To reveal the origin of this observation, we performed a Gaussian deconvolution analysis, revealing that the spectra consist of green, blue, and UV bands, respectively, regardless of the measurement temperature. As an example, Figure 4(b) presents the PL spectrum at 18.8 K with a Gaussian fitting. We notice that the intensity of the green emission band progressively decreases with increasing measurement temperature, with its peak position remaining unchanged (Figure 4(c)). Presumably, this observation is

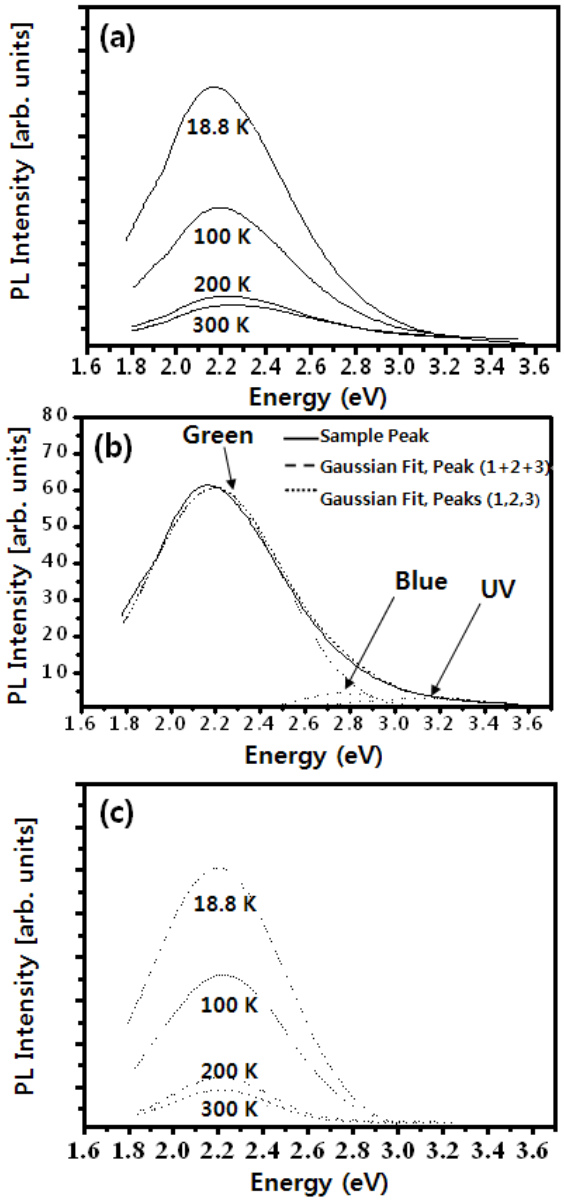

Fig. 4. (a) Temperature-dependent PL of MgO/ZnO core-shell nanowires sputtered for 8 min. (b) PL spectrum at 18.8 K with a Gaussian fitting analysis. (c) Variation of the green-emission bands (Gaussian functions) with varying measurement temperature.

ascribed to the freezeout of phonons and to the quenching of nonradiative recombination processes [30].

III. CONCLUSION

In summary, fabrication of MgO-core/ZnO-shell nanowires was demonstrated, in which outer layers were deposited via RF sputtering. The morphologies, microstructures, and compositions of the resulting core-shell nanowires were investigated using SEM, XRD, TEM, and EDX. The PL measurements with a Gaussian fitting show blue, green and UV emission bands. At 298 K, the peak intensity ratio (green (2.4 eV)/ UV (3.2 eV)) decreased with increasing ZnO shell thickness. Also, we reveal that the intensity of the green emission increased with decreasing measurement temperature in the range of 18.8 K to 300 K. This approach can be applied to prepare and analyze various coaxial nanocables sheathed by a plasma sputtering process.

ACKNOWLEDGMENTS

This work was supported by a Korea Research Foundation grant funded by the Korean Government (MOEHRD) (KRF-2007-521-D00216). The main calculations were performed by the supercomputing resources of the Korea Institute of Science and Technology Information (KISTI).

REFERENCES

[1] S. Iijima, Nature **354**, 56 (1991)
[2] J. Hu, T. W. Odom and C. M. Lieber, Acc. Chem. Res. **32**, 435 (1999)
[3] H. W. Kim, S. H. Shim, J. W. Lee and C. Lee, J. Korean Phy. Soc. **51**, 204 (2007).
[4] S. Park, H. Kim, J. W. Lee, H. W. Kim and C. Lee, J. Korean Phy. Soc. **53**, 657 (2008).
[5] H. K. Seong, H. N. Jeong, R. Ha, J. C. Lee, Y. M. Sung and H. J. Choi, Met. Mater. Int. **14**, 354 (2008).
[6] H. K. Seong, M. H. Kim, H. J. Choi, Y. J. Choi and J. G. Park, Met. Mater. Int. **14**, 477 (2008).
[7] S-L. Zhang, S-M. Park, J-O. Lim and J-S. Huh, Met. Mater. Int. **14**, 621(2008).
[8] J. Y. Park and S. S. Kim, Met. Mater. Int. **14**, 357 (2008).
[9] S. H. C. Liang and I. D. Gay, J. Catal. **101**, 293 (1986).
[10] A. N. Copp, Am. Ceram. Soc. Bull. **74**, 135 (1995).
[11] P. D. Yang and C. M. Lieber, Science **273**, 1836 (1996).
[12] G. P. Summers, T. M. Wilson, B. T. Jeffries, H. T. Tohver, Y. Chen and M. M. Abraham, Phys. Rev. B **27**, 1283 (1983).
[13] G. H. Rosenblatt, M. W. Rowe, G. P. Williams, Jr., R. T. Williams and Y. Chen, Phys. Rev. B **39**, 10309 (1989).
[14] J. L. Grant, R. Cooper, P. Zeglinski and J. F. Boas, J. Chem. Phys. **90**, 807 (1989).
[15] R. Z. Ma and Y. Bando, Chem. Phys. Lett. **370**, 770 (2003)
[16] Y. Q. Zhu, W. K. Hsu, W. Z. Zhou, M. Terrones, H. W. Kroto and D. R. M. Walton, Chem. Phys. Lett. **347**, 337 (2001)
[17] J. Grabowska, K. K. Nanda, E. McGlynn, J-P. Mosnier, M. O. Henry, A. Beaucamp and A. Meaney, J. Mater. Sci.: Mater. El. **16**, 397 (2005).
[18] G-C. Yi, C. Wang and W. I. Park, Semicond. Sci. Technol. **20**, S22 (2005).

[19] J. Zhou and N. S. Xu, Adv. Mater. **18**, 2432 (2006).
[20] Y. J. Zeng, Z. Z. Ye, F. Liu, D. Y. Li, Y. F. Lu, W. Jaeger, H. P. He, L. P. Zhu, J. Y. Huang and B. H. Zhao, Cryst. Growth Des. **9**, 263 (2009).
[21] N. O. V. Park, H. J. Snaith, C. Ducati, J. S. Bendall, L. Schmidt-Mende and M. E. Welland, Nanotechnology **19**, 465603 (2008).
[22] H. W. Kim and N. H. Kim, Mater. Sci. Eng. B **103**, 297 (2003)
[23] Y. Hao, G. Meng, C. Ye, X. Zhang and L. Zhang, J. Phys. Chem. B **109**, 11204 (2005).
[24] D. C. Reynolds, D. C. Look, B. Jogai, C. W. Litton, T. C. Collins, W. Harsch and G. Cantwell, Phys. Rev. B **57**, 12151 (1998).
[25] S. W. Jung, W. I. Park, H. D. Cheong, G-C. Yi, H. M. Jang, S. Hong and T. Joo, Appl. Phys. Lett. **80**, 1924 (2002).
[26] P. Yang, H. Yan, S. Mao, R. Russo, J. Johnson, R. Saykally, N. Morris, J. Pham, R. He and H-J. Choi, Adv. Funct. Mater. **12**, 323 (2002).
[27] Q. Wan, Z. T. Song, W. L. Liu, C. L. Lin and T. H. Wang, Nanotechnology **15**, 559 (2004).
[28] M. H. Huang, Y. Wu, H. Feick, N. Tran, E. Weber and P. Yang, Adv. Mater **13**, 113 (2001).
[29] E. S. Kim, H. S. Kang, J. S. Kang, J. H. Kim and S. Y. Lee, Appl. Surf. Sci. **186**, 474 (2002).
[30] L. E. Greene, M. Law, J. Goldberger, F. Kim, J. C. Johnson, Y. Zhang, R. J. Saykally and P. Yang, Angew. Chem. Int. Ed. **42**, 3031 (2003).